

Exploring the Effect of Polymer Addition to the Room Temperature Synthesis of Colloidal Lead Halide Perovskite for Better Stability, Higher Passivation, and More Uniform Particle Size

Elshaimaa Darwish,* Jack Elia, Mirosław Batentschuk, Andres Osvet, and Christoph J. Brabec*

In recent years, metal halide perovskites have emerged as a promising alternative to existing semiconductor materials in many applications due to its appealing properties. Despite perovskite huge potentials in many applications, they are still suffering from different kinds of stability issues that are hindering their marketability. Several attempts to stabilize perovskites including polymer encapsulations and inclusions of perovskite materials into polymer matrices due to the stability against moisture that the polymer can offer. Nevertheless, the polymer is acting as an unreactive component without any role into enhancing the optical properties of the studies metal halide perovskite. This study examines the incorporation of the polymer BUTVAR (polyvinyl butyral [PVB]) in the production of various perovskite structures at room temperature: CsPbBr_3 , Cs_2PbBr_5 , FAPbBr_3 , and MAPbBr_3 . The study demonstrates that the incorporation of the polymer solution enhances the optical characteristics and improves the shape uniformity of the resultant perovskite material without altering the inherent structure of the original perovskite material. Furthermore, it improves the durability of the acquired particles against UV irradiation.

perovskites with ABX_3 stoichiometry ($\text{A} = \text{CH}_3\text{NH}_3^+$, $\text{CH}(\text{NH}_2)_2^+$, Cs^+ , $\text{B} = \text{Pb}^{2+}$ or Sn^{2+} , and $\text{X} = \text{Cl}^-$, Br^- or I^-) have emerged as promising alternatives to replace existing semiconductor materials. These perovskites exhibit improved device performance and possess distinctive optical characteristics. The optical characteristics are a consequence of the efficient transport of electrons and holes, remarkable absorption coefficients throughout a wide range of wavelengths (e.g., 380–750 nm),^[14] and exceptional quantum yields (QYs) for photoluminescence (PL).^[15] Therefore, this property makes the material extensively appropriate for optoelectronic and photovoltaic applications. Moreover, the economical nature of material synthesis makes perovskite materials a feasible alternative for existing semiconductor materials.^[16]

Despite perovskite materials' considerable potential for optic and electrical applications across a diverse range of domain sizes, their poor stability against moisture, UV-vis irradiation, and heat limits their practical use in devices.

Small molecule ligands are widely employed in the controlled production of perovskite nanocrystals (NCs).^[12,17–19] It has been proven that implementing certain ligands enhances the stability of perovskite NCs. The inclusion of these ligands has the potential to improve the QY and PL characteristics, thereby bolstering the colloidal solution's general stability. The ionic structure of perovskite crystals, combined with the dynamic nature of small molecule ligand binding to the perovskite surface, continues to impose challenges related to agglomeration and diminished stability against environmental variables.^[20]


It has been demonstrated that postsynthetic encapsulation of ABX_3 perovskites in polymer matrix enhances long-term stability while preserving optical characteristics.^[21–27] The application of a thin, passivating layer of poly(methyl methacrylate) was shown to effectively inhibit moisture absorption and sustain the high-power conversion efficiency (PCE) of manufactured solar cells.^[27] Furthermore, poly(styrene) was employed as a capping layer to fabricate an inner-encapsulated perovskite solar cell with improved PCE. In both instances, the polymers used in the

1. Introduction

In several fields such as solar water splitting,^[1] photovoltaics,^[2–5] light-emitting diodes (LEDs),^[6–8] photodetectors,^[9,10] imaging,^[11] and optical displays,^[12,13] hybrid organic/inorganic halide

E. Darwish, J. Elia, M. Batentschuk, A. Osvet, C. J. Brabec
Materials for Electronics and Energy Technology (i-MEET)
Friedrich-Alexander-Universität Erlangen-Nürnberg
Martensstraße 7, 91058 Erlangen, Germany
E-mail: elshaimaa.darwish@fau.de; christoph.brabec@fau.de

C. J. Brabec
Helmholtz Institute Erlangen-Nürnberg for Renewable Energy (HI-ERN)
Forschungszentrum Jülich GmbH
Immerwahrstraße 2, 91058 Erlangen, Germany

 The ORCID identification number(s) for the author(s) of this article can be found under <https://doi.org/10.1002/adem.202402713>.

© 2025 The Author(s). Advanced Engineering Materials published by Wiley-VCH GmbH. This is an open access article under the terms of the Creative Commons Attribution License, which permits use, distribution and reproduction in any medium, provided the original work is properly cited.

DOI: 10.1002/adem.202402713

fabrication of composite perovskite/polymer solar cells enhance the device's performance by serving as an inert constituent for previously produced crystals, thereby increasing the overall material's stability. In addition, Wang et al. described a method of microencapsulation to prepare evenly distributed organic–inorganic hybrid perovskite NCs in polymer matrices by utilizing a polymer-solvent swelling–deswelling phenomena. The PL efficiency of the film remained constant when exposed to boiling water for a period of 60 days.^[26] The studies conducted by Wei et al. Xuan et al. and Papagiorgis et al. demonstrated that perovskite NCs were produced by hot injection and integrated with small molecule ligands oleylamine (OAm) and oleic acid (OA) in various polymer matrixes. These investigations demonstrated that encapsulating the NCs with a polymer after synthesis reduced their degradation and, in certain instances, enhanced the efficacy of photoconversion. Nevertheless, the incorporation and distribution of perovskites in the majority of polymers rely on the assumption that polymers are nonreactive constituents, therefore restricting the potential for improving the optical characteristics of the materials by cooperative interactions between the polymer and inorganic components.^[22,23,25] Furthermore, Manav et al. have used polymer coating/encapsulation with CsPbBr₃ nanoparticles as a way of enhancing the water stability of the perovskite nanoparticles and to limit the lead toxicity at the same time for bioimaging application.^[28]

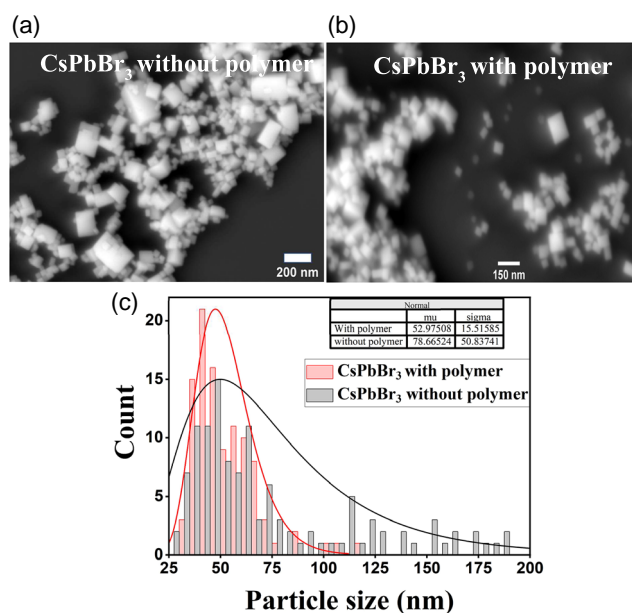


Figure 2. a) SEM image of CsPbBr₃ synthesized without the polymer. b) SEM image of CsPbBr₃ synthesized with the addition of polymer. c) Histogram comparing the particle size distribution of each kind of the particles with and without the polymer.

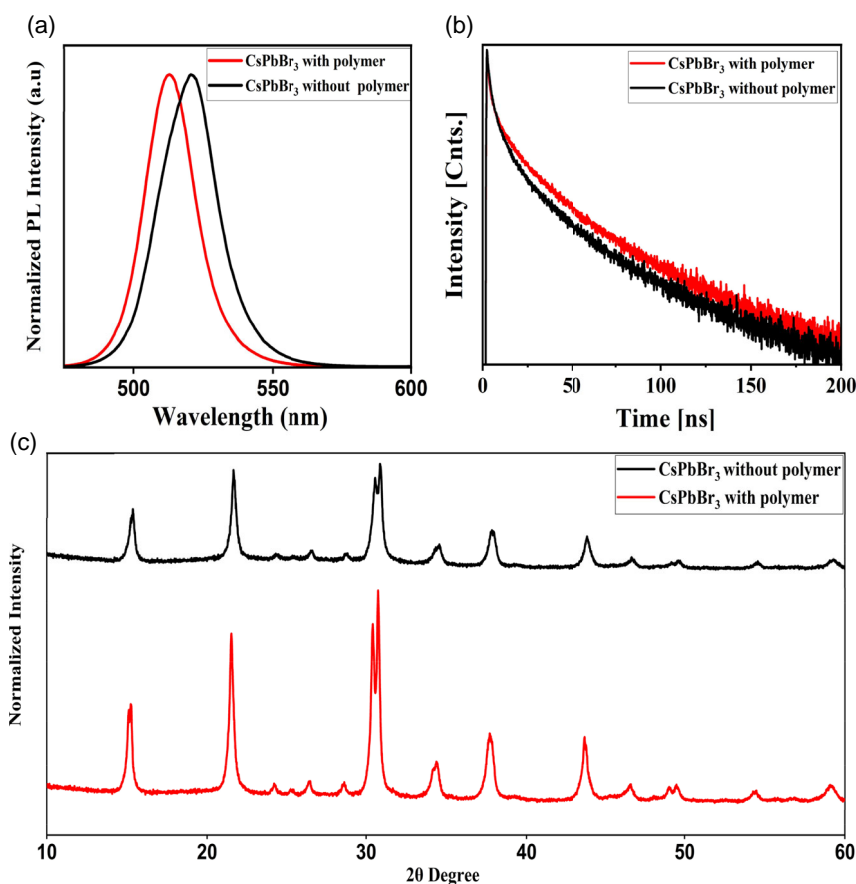


Figure 1. a) Normalized PL emission spectrum of CsPbBr₃ with and without the addition of the polymer; the emission is recorded at excitation 365 nm. b) TrPL decay of CsPbBr₃ with and without the addition of the polymer. c) XRD spectrum of CsPbBr₃ with and without polymer.

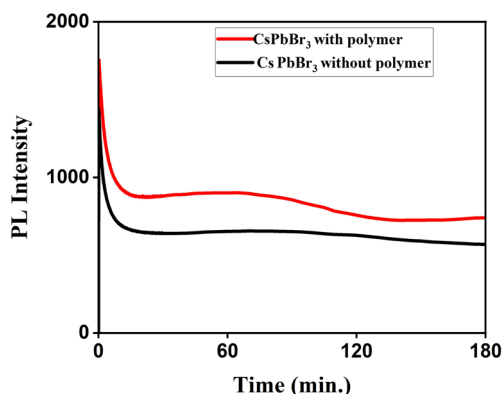


Figure 3. Film degradation of CsPbBr₃ with and without polymer; the degradation was performed with LED light of 375 nm wavelength and power of 250 mW; the emission was recorded at the peak maximum of each sample for 180 min.

Moreover, Jiang et al. have tested a few types of polymers to be used as dopant for perovskites films used in solar cells, which resulted in enhancement in the film morphology and device stability; their study focused on MAPbI₃.^[29] In addition, another study by Arivunithi et al. used a side-chain liquid crystalline polymer to be incorporated as a dopant into the perovskite film;

doped films have showed improved air stability and decreased trap state density. Doped perovskite films were used to achieve perovskite solar cells with higher efficiency and long-term stability. They conducted that the side-chain liquid crystalline polymer acted as a bridge between grains for effective charge transfer which enhanced the final device stability.^[30]

In our previous study,^[31] we found that the addition of polymer to the precursor solution during the colloidal synthesis process of Cs₄PbBr₆ has significantly enhanced the purity and the QY of the desired product, which also enhanced the performance of the Cs₄PbBr₆ as a downshifting layer when compared to the same particles prepared without the addition of the polymer. The addition of the polymer to the precursor solution was inspired by previous studies,^[32,33] where they added the polymer solution during the film fabrication, which enhanced the film transparency and thus the solar cells performance. However, we adopted the polymer solution incorporation differently to be used during the colloidal synthesis process.

Herein, we further continue our study to include the investigation of the addition of the same polymer (BUTVAR B-98 (polyvinyl butyral [PVB])) to the synthesis of several perovskite structures at room temperature: CsPbBr₃, Cs₂PbBr₅, FAPbBr₃, and MAPbBr₃. Our study proves the ability of the addition of the polymer solution to enhance the optical properties and increase the shape uniformity of the obtained perovskite material without

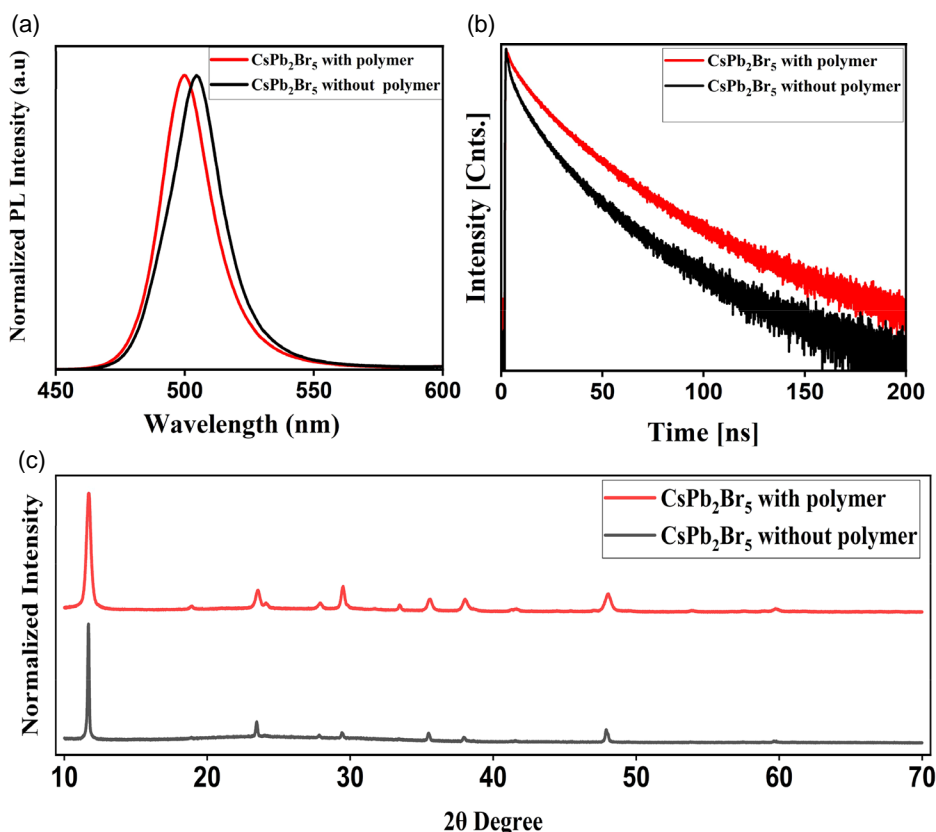


Figure 4. a) Normalized PL emission spectrum of CsPb₂Br₅ with the polymer (red line) and without the polymer (black line); the emission is recorded at excitation 365 nm. b) TrPL decay of CsPb₂Br₅ with the polymer (red line) and without the addition of the polymer (black line). c) XRD spectrum of CsPb₂Br₅ with the polymer (red line) and without polymer (black line).

changing the native structure of the starting perovskite material in addition to enhancing the stability of the obtained particles against UV irradiation.

2. Results and Discussion

CsPbBr₃ was synthesized at room temperature using the reverse microemulsion method.^[34] In order to study the effect of the polymer addition to the perovskite particles synthesis, two samples of each material were prepared: one without the polymer following the original synthesis recipe and another one after mixing the polymer with the precursor containing solution. Each sample is characterized optically via measuring the PL emission and structurally via recording the X-ray diffraction (XRD) spectrum of both of the samples before and after the addition of polymer. As shown in **Figure 1**, the addition of the BUTVAR polymer to the CsPbBr₃ resulted in a blueshift of the PL emission spectrum toward a shorter wavelength, indicating a reduction in particle size (**Figure 1a**). Moreover, the time-resolved PL (TrPL) (**Figure 1b**) shows an increase in the decay time for the particles synthesized with the polymer. This increase in the decay time suggests that the excitons in the polymer-modified particles have a longer lifetime, which can be attributed to reduced nonradiative recombination processes due to surface defect passivation. The enhancement in the PL QY (PLQY) of 10% for the particles prepared with the polymer compared to those synthesized without it further supports this conclusion. The increase in both TrPL decay time and PLQY indicates that the polymer acts as a passivation layer, effectively reducing surface defects that typically act as nonradiative recombination centers.

Furthermore, the XRD spectrum (**Figure 1c**) shows no significant difference in the crystal structure of the particles before and after the addition of the polymer, confirming that the polymer addition did not alter the material's intrinsic structure. The observed effects are thus attributed to surface passivation and the additional confinement provided by the polymer.

In addition to the optical characterization of the particles, scanning electron microscopy (SEM) images were also recorded for the CsPbBr₃ particles with and without addition of the polymer as shown in **Figure 2**. **Figure 2a** is an SEM image of the particles synthesized without the polymer, while **Figure 2b** is an SEM image of the particles synthesized with the polymer added to the precursor containing solution. From both images it could be visually observed that the addition of the polymer in the synthesis caused the overall particles size to be smaller and more uniform. **Figure 2c** is a histogram comparing the sizes of both samples with and without the polymer; each image was processed with ImageJ software and the sizes of the particles were measured using the same software. From the histogram it could be seen that the average particle size in case of particles synthesized without polymer is 78.6 nm, while the average particle size in case of particles synthesized with polymer is 52.9 nm. Moreover, the graph in **Figure 2c** is showing a wider range of particle sizes distribution in case of the particles without polymer, while the sizes distribution in case of particles with polymer is getting narrower.

In order to test how the addition of the polymer will affect the material photostability, a degradation experiment of the films of both kind of particles with and without the polymer; as shown in **Figure 3**; in case of CsPbBr₃ prepared without the polymer the emission shows an abrupt decay at the beginning of degradation followed by a steady emission till the end, while in the case of the sample prepared with the addition of the polymer the emission decay in the beginning is less sharp than the other sample and there is an observed self-healing behavior of the emission afterward.

The second investigated lead halide perovskite is CsPb₂Br₅, which was also synthesized at room temperature using the reverse microemulsion method following the previously published method.^[34] To synthesize the samples with polymer, 20 μ L of 0.1 g mL⁻¹ BUTVAR (PVB) polymer stock solution was added to the PbBr₂ containing solution following the addition of the OA and OAm ligands as described in the Experimental Section. In order to understand the effect that the polymer addition is causing to the CsPb₂Br₅ particles, two samples were prepared: one with the addition of the polymer and one without the polymer following the published synthesis method and both were characterized optically and structurally in addition to taking the SEM images of both samples with and without the polymer. Finally, films of each sample were degraded under UV light to see the effect of the polymer addition on the UV stability of the material.

As shown in **Figure 4**; the same trend that was observed in case of CsPbBr₃ is also observed in case of CsPb₂Br₅. Mainly, the sample with the polymer is showing a blueshift to shorter emission wavelength, as shown in **Figure 4a**, which is an indication of the size reduction of the nanoparticles. Also, the TrPL decay is showing an increment in the decay time in case of the particles synthesized with the polymer when compared to the particles

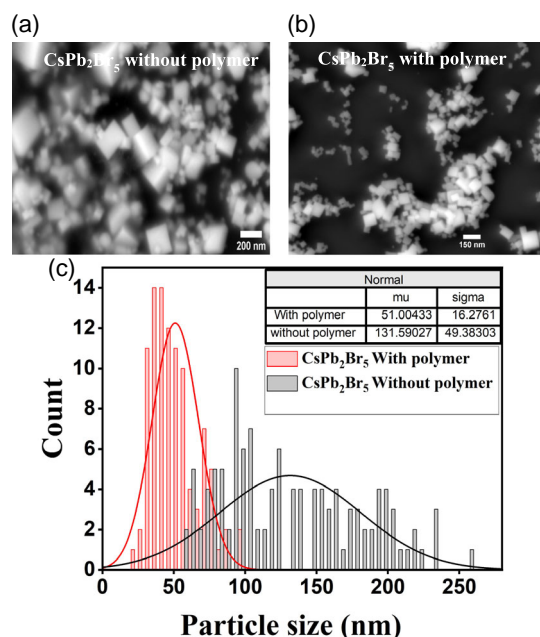


Figure 5. a) SEM image of CsPb₂Br₅ without polymer. b) SEM image of CsPb₂Br₅ with polymer. c) Histogram comparing the particle sizes of each sample and calculating the average particle size in each of them.

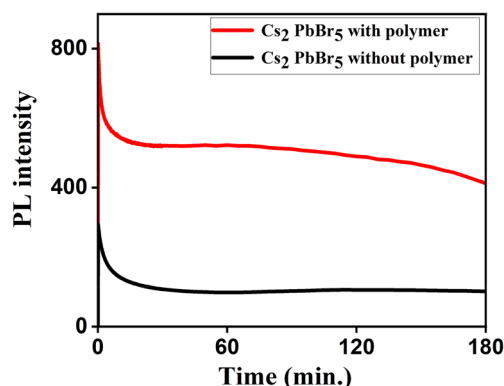


Figure 6. Film degradation of CsPb_2Br_5 with polymer (red line) and without polymer (black line); the degradation was performed with LED light of 375 nm wavelength and power of 250 mW; the emission was recorded at the peak maximum of each sample for 180 min.

synthesized without the polymer as shown in Figure 4b. As a result of the surface passivation, the polymer is adding to the perovskite nanoparticles. The PLQY of the particles with the polymer is showing an increment of 28% when compared to the particles without the polymer. Moreover, the XRD curves in Figure 4c of the particle with and without polymers are identical, which proves that the observed effects are due to the surface passivation of the particles without changing the particle's native structure nor forming new species as a result of the polymer addition.

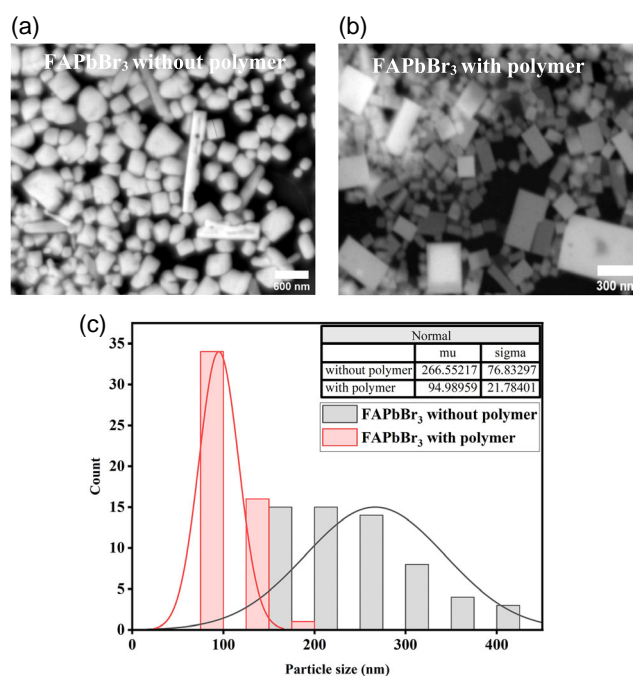


Figure 8. a) SEM image of FAPbBr_3 synthesized without the polymer (scalebar 600 nm). b) SEM image of FAPbBr_3 synthesized with the addition of polymer (scalebar 300 nm). c) Histogram comparing the particle size distribution of each kind of the particles with and without the polymer.

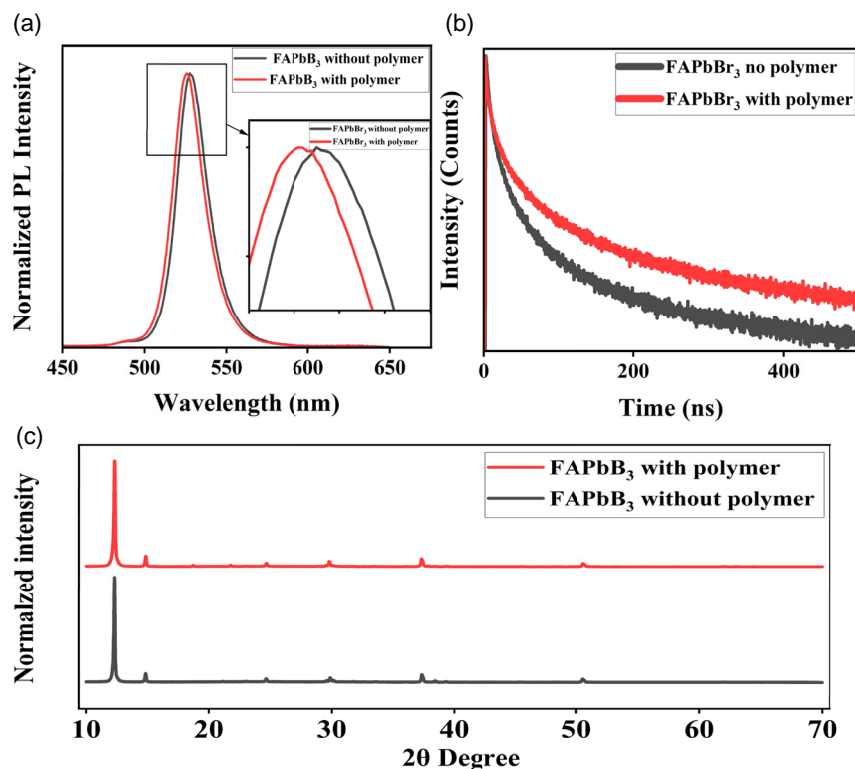


Figure 7. a) Normalized PL emission spectrum of FAPbBr_3 with and without the addition of the polymer; the emission is recorded at excitation 365 nm. b) TrPL decay of FAPbBr_3 with and without the addition of the polymer. c) XRD spectrum of FAPbBr_3 with and without polymer.

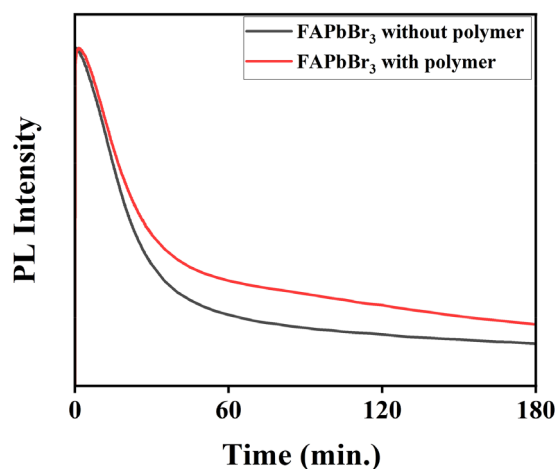


Figure 9. Film degradation of FAPbBr₃ with polymer (red line) and without polymer (black line); the degradation was performed with LED light of 375 nm wavelength and power of 250 mW; the emission was recorded at the peak maximum of each sample for 180 min.

Figure 5 is showing the SEM images of CsPb₂Br₅ with and without polymer from Figure 5a,b. It could be visually observed that the particles synthesized with addition of polymer are

smaller in size and with less variation in the size; calculations offered by the histogram in Figure 5c are a further confirmation that the average particle size in case of particles without polymer is around 131.5 nm, while the average particle size in case of the particles with polymer is around 51 nm.

The stability against UV-light irradiation was tested as well for both samples with and without polymer as shown in Figure 6. It is also observed that the CsPb₂Br₅ containing polymer is having a higher emission and is also showing higher self-healing which is shown by the emission increment at some points after UV-light irradiation.

Moreover, the effect of polymer addition to the precursor solution was also examined in case of organic–inorganic metal halide perovskite at room temperature. Mainly, FAPbBr₃ and MAPbBr₃ were both synthesized using the LARF method and for each material a sample without the polymer using the original previously published method was taken as a reference.

FAPbBr₃ was synthesized according to the previously published protocol;^[35] for the sample containing polymer, 10 μ L of the polymer stock solution was added to the precursor and ligand containing solution and mixed by sonication prior to the solution injection into the chloroform antisolvent. Optical and structural characterization results in Figure 7 are showing similar effect due to the polymer addition as shown in case of both all-inorganic metal halide perovskites discussed

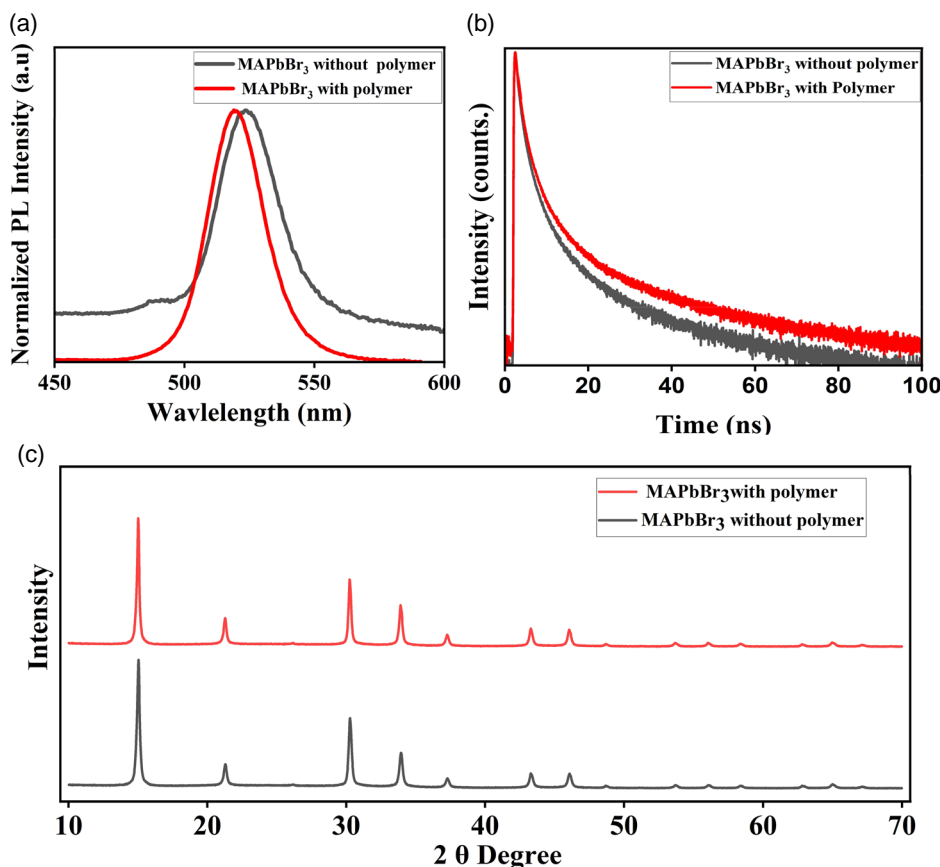


Figure 10. a) Normalized PL emission spectrum of MAPbBr₃ with and without the addition of the polymer; the emission is recorded at excitation 365 nm. b) TrPL decay of MAPbBr₃ with and without the addition of the polymer. c) XRD spectrum of MAPbBr₃ with and without polymer.

previously (CsPbBr_3 , CsPb_2Br_5). Therefore, we can also conclude that the polymer acted as a surface passivation layer in the case of FAPbBr_3 as well.

Furthermore, the SEM images at **Figure 8a,b** are showing the particle size reduction after the polymer addition. The histogram in **Figure 8c** is showing that the average particle size has reduced from 266.5 nm in case of the particles without polymer to 94.9 nm in case of the particles with polymer, with a narrower range of particle size distribution in case of FAPbBr_3 synthesized with the addition of polymers.

Figure 9 is showing the film degradation of FAPbBr_3 under UV-light irradiation; higher resistance is observed for the FAPbBr_3 with polymer (red line) when compared to the one without polymer (black line).

Same systematic investigation was used to examine the effect of the polymer addition to the MAPbBr_3 synthesis. **Figure 10a** is showing that the addition of polymer caused the PL emission peak to be shifted to a shorter wavelength which indicates more confinement; also, the increment of the decay lifetime in **Figure 10b** is indicating more surface passivation and less traps and the XRD in **Figure 10c** is showing that both curves with and without polymer are identical which confirm that polymer addition did not change the structure of the material.

Furthermore, the SEM images at **Figure 11a,b** are showing the particle size reduction after the polymer addition. The histogram in **Figure 11c** is showing that the average particle size has reduced from 36 nm in case of the particles without polymer to 28 nm in case of the particles with polymer, with a narrower range of particle size distribution in case of MAPbBr_3 synthesized with the addition of polymers.

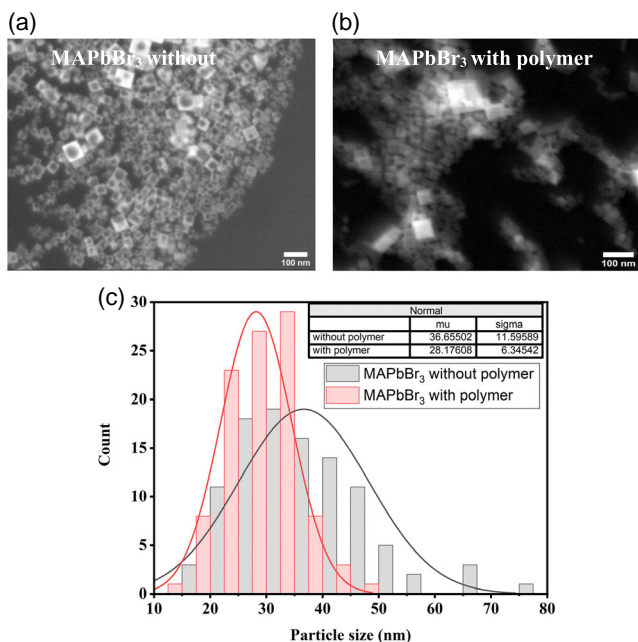


Figure 11. a) SEM image of MAPbBr_3 synthesized without the polymer. b) SEM image of MAPbBr_3 synthesized with the addition of polymer. c) Histogram comparing the particle size distribution of each kind of the particles with and without the polymer.

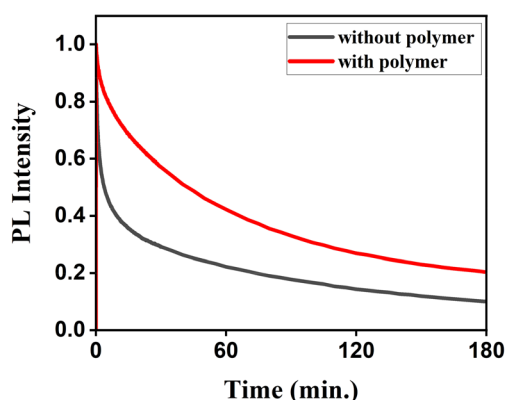


Figure 12. Film degradation of MAPbBr_3 with polymer (red line) and without polymer (black line); the degradation was performed with LED light of 375 nm wavelength and power of 250 mW; the emission was recorded at the peak maximum of each sample for 180 min.

The UV-light stability was also tested for MAPbBr_3 . **Figure 12** is showing that the sample with polymer had more resistance against UV-light irradiation with less abrupt degradation in the beginning of the irradiation time unlike the sample without the polymer.

3. Conclusion

In this work, we tested the effect of adding BUTVAR polymer to the precursor solution during the synthesis of lead halide perovskite at room temperature. Several types of lead halide perovskite materials were examined in this study: CsPbBr_3 , CsPb_2Br_5 , FAPbBr_3 , and MAPbBr_3 .

A constant trend was observed in case of all the studied materials that polymer addition helped in decreasing the particle size, adding more confinement, and decreasing the surface traps, thus enhancing the PLQY. Moreover, we believe that the particles synthesized with the polymer are more easily dispersed into the binder solution of the same polymer which is resulting in more stable inks for optical applications that require dispersing light converting materials into transparent and inert polymer binder.

4. Experimental Section

Materials: Lead (II) bromide (PbBr_2 , 98%), cesium carbonate (Cs_2CO_3 , 99%), *N,N*-dimethylformamide (DMF, 99.8%), OAm (90%), anhydrous *n*-hexane (99.98%), chloroform (>99%), HBr (48%), and polyvinyl butyral (BUTVAR B-98) were purchased from Sigma-Aldrich. OA (97%) was purchased from VWR Chemicals. Formamidinium bromide (FABr) and methylammonium bromide (MABr) were purchased from Great Cell Solar.

CsPbBr_3 Synthesis: Perovskite NCs were synthesized using a room temperature method that was previously published.^[34] Briefly, the precursors Cs-oleate was prepared independently; 2.25 g of Cs_2CO_3 and 21.5 mL of OA were mixed and degassed at 130 °C in a vacuum for 1 h to produce a yellowish stock of Cs-oleate precursor. Synthesis of CsPbBr_3 NCs was achieved by introducing 25 μL of Cs-oleate precursor, 10 mL of *n*-hexane, and 5 mL of OA into a 50 mL flask. A solution containing 11.01 mg of PbBr_2 dispersed in 1 mL DMF (0.03M PbBr_3 , DMF), 2 μL of

HBr (48%), 0.1 mL of OA, and 0.05 mL of OAm was produced in a separate bottle and added to the first flask while stirring vigorously. Following the observed color change from white to green within 10 min, the NCs were collected by centrifugation at 8000 revolutions per minute for 3 min. The NCs were then dispersed in 2 mL of chloroform for further analysis.

For the samples with polymer, a stock solution of BUTVAR (PVB) in DMF was prepared with the concentration of 0.1 g mL^{-1} ; 20 μL of the polymer solution was mixed with the PbBr_2 solution and the OA and OAM before the addition to the Cs-Oleate containing solution.

CsPb₂Br₅ Synthesis: CsPb₂Br₅ NC synthesis was done following the same method used for CsPbBr₃, with changing the amount of Cs-oleate precursor used to be 10 μL and the HBr to be 1 μL . Briefly, the synthesis of CsPb₂Br₅ NCs was achieved by introducing 10 μL of Cs-oleate precursor, 10 mL of *n*-hexane, and 5 mL of OA into a 50 mL flask. A solution containing 11.01 mg of PbBr₂ dispersed in 1 mL DMF (0.03M PbBr₃, DMF), 1 μL of HBr (48%), 0.1 mL of OA, and 0.05 mL of OAm was produced in a separate bottle and added to the first flask while stirring vigorously. Following the observed color change from white to green within 10 min, the NCs were collected by centrifugation at 8000 revolutions per minute for 3 min. The NCs were then dispersed in 2 mL of chloroform for further analysis. XRD analysis was used later to confirm the successful synthesis process of the required stoichiometry.

For the samples with polymer, a stock solution of BUTVAR (PVB) in DMF was prepared with the concentration of 0.1 g mL^{-1} ; 20 μL of the polymer solution was mixed with the PbBr_2 solution and the OA and OAM before the addition to the Cs-Oleate containing solution.

FAPbBr₃ Synthesis: Was synthesized at room temperature using a previously published method.^[35] Briefly, a 0.1 mM solution was formed by dissolving FABr (0.0112 g, 0.1 mmol) and PbBr₂ (0.0367, 0.1 mmol) in 1 mL of DMF. Next, 20 μL of OA and 20 μL of OAm were introduced. Following that, 200 μL of this combination was introduced into 6 mL of chloroform. Immediate formation of bright green-emitting NCs occurred. Purification was achieved by precipitating the resulting nanocrystal solution with 3 mL of toluene and then centrifuging it at 9000 rpm for 2 min. The resulting NCs were completely dispersed in 3 mL of nonpolar volatile solvents including hexane, toluene, chloroform, and others. All experiments in this work used chloroform.

For the samples with polymer, a stock solution of BUTVAR (PVB) in DMF was prepared with the concentration of 0.1 g mL^{-1} ; 20 μL of the polymer solution was mixed with the precursor containing solution and the OA and OAM before the addition to the antisolvent.

MAPbBr₃ Synthesis: Was synthesized at room temperature using a previously published method^[36] with slight modifications. Briefly, CH₃NH₃Br (0.0112 g, 0.1 mmol) and PbBr₂ (0.0367, 0.1 mmol) were dissolved in 1 mL of DMF to produce a 0.1 mM solution. Then, 20 μL of OA and 20 μL of OAm were added. Furthermore, 200 μL of this mixture was introduced into 6 mL of either toluene or chloroform. Instantaneous formation of bright emitting nanoparticles was observed. Purification was achieved by precipitating the resulting particles solution with 3 mL of toluene and then centrifuging it at 9000 rpm for 2 min. The resulting nanoparticles were dispersed in chloroform.

For the samples with polymer, a stock solution of BUTVAR (PVB) in DMF was prepared with the concentration of 0.1 g mL^{-1} ; 20 μL of the polymer solution was mixed with the precursor containing solution and the OA and OAM before the addition to the antisolvent.

Characterizations: XRD: XRD studies were conducted using a Panalytical X'pert powder diffractometer with a Cu K α radiation intensity of 1.5406 \AA , employing a typical ex situ Bragg–Brentano geometry. For each measurement, a concentrated chloroform solution containing NCs was applied by drop casting onto a glass substrate.

Characterizations: Optical Characterization: The emission spectra of the nanocrystalline dispersions were determined using a Jasco FP8500 spectrofluorometer. Fluorometer's wavelength-dependent spectral responsivity was accounted for in the correction of the emission spectra.

Characterizations: The Quantum Efficiency of PL: The quantum efficiency of PL was quantitatively determined using the methodology described by de Mello et al.^[24] The samples were affixed on a 3.3 inch integrating sphere, which was connected to an Avantes spectrometer using fiber

optical cables. Spectra of the samples, stimulated by a 405 nm laser diode, were adjusted to account for the equipment's spectral sensitivity, which was evaluated using a calibrated Xe lamp from Hamamatsu.

Characterizations: TrPL decay: The decay curves of PL were measured using a Fluotime 300 spectrometer manufactured by PicoQuant GmbH. The measurements were performed by stimulating the sample using a pulsed diode laser that emitted the light at a wavelength of 402 nm. The energy flow density measure $0.5 \mu\text{J}$ per square centimeter.

Characterizations: SEM Scanning Techniques: The SEM images were captured using a Carl Zeiss field-emission microscope operating at a voltage of 5 kV. Each measurement involved drop casting a diluted chloroform solution of NCs onto a silicon wafer substrate and then annealing at 60°C to evaporate the solvent.

Characterizations: Photostability Test/Degradation: In order to perform the degradation of the samples, an LED lamp of wavelength 375 nm was installed inside the sample chamber of the Jasco FP-8500 fluorometer as an excitation source. The sample in form of a film was placed inside the sample holder of the fluorometer and PL intensity at the peak wavelength of the sample was recorded by Jasco FP-8500 during irradiation.

Supporting Information

Supporting Information is available from the Wiley Online Library or from the author.

Acknowledgements

All authors gratefully acknowledge the German Research Foundation (Deutsche Forschungsgemeinschaft) for the framework of GRK2495/E. E.D. gratefully acknowledges funding of the Erlangen Graduate School in Advanced Optical Technologies (SAOT) by the Bavarian State Ministry for Science and Art. Also, she gratefully acknowledges the German Academic Exchange Service (DAAD) for the offered research grant for the doctoral program. E.D. would also like to show her special sincere gratitude to the Bavarian Equal Opportunities Sponsorship—Realisierung von Chancengleichheit von Frauen in Forschung und Lehre (FFL)—Realization of Equal Opportunities for Women in Research and Teaching.

Open Access funding enabled and organized by Projekt DEAL.

Conflict of Interest

The authors declare no conflict of interest.

Author Contributions

Elshaimaa Darwish: conceptualization (supporting); formal analysis (lead); investigation (lead); methodology (lead); writing—original draft (lead); writing—review editing (supporting). **Jack Elia:** data curation (supporting). **Andres Osvet:** supervision (supporting); writing—review editing (lead). **Mirosław Batentschuk:** project administration (lead); supervision (supporting); writing—review editing (supporting). **Christoph J. Brabec:** conceptualization (lead); supervision (lead); writing—review editing (lead).

Data Availability Statement

The data that support the findings of this study are openly available in [NAME] at [DOI], reference number [REF].

Keywords

perovskite nanocrystals, perovskite nanoparticles higher passivation, perovskite stability, polymer addition to perovskite nanocrystal synthesis, room temperature synthesis

Received: November 18, 2024

Revised: March 7, 2025

Published online: April 4, 2025

- [1] E. Edwardes Moore, V. Andrei, S. Zacarias, I. A. C. Pereira, E. Reisner, *ACS Energy Lett.* **2020**, 5, 232.
- [2] A. Dey, J. Ye, A. De, E. Debroye, S. K. Ha, E. Bladt, A. S. Kshirsagar, Z. Wang, J. Yin, Y. Wang, L. N. Quan, F. Yan, M. Gao, X. Li, J. Shamsi, T. Debnath, M. Cao, M. A. Scheel, S. Kumar, J. A. Steele, M. Gerhard, L. Chouhan, K. Xu, X.-G. Wu, Y. Li, Y. Zhang, A. Dutta, C. Han, I. Vincon, A. L. Rogach, et al., *Am. Chem. Soc.* **2021**, 15, 10775.
- [3] J. Burschka, N. Pellet, S.-J. Moon, R. Humphry-Baker, P. Gao, M. K. Nazeeruddin, M. Grätzel, *Nature* **2013**, 499, 316.
- [4] R. Fickler, R. Lapkiewicz, W. N. Plick, M. Krenn, C. Schaeff, S. Ramelow, A. Zeilinger, *Science* **2012**, 338, 640.
- [5] M. G. A. Lapotre, R. C. Ewing, M. P. Lamb, W. W. Fischer, J. P. Grotzinger, D. M. Rubin, K. W. Lewis, M. J. Ballard, M. Day, S. Gupta, S. G. Banham, N. T. Bridges, D. J. Des Marais, A. A. Fraeman, J. A. Grant, K. E. Herkenhoff, D. W. Ming, M. A. Mischna, M. S. Rice, D. Y. Sumner, A. R. Vasavada, R. A. Yingst, *Science* **2016**, 353, 55.
- [6] L. Protesescu, S. Yakunin, M. I. Bodnarchuk, F. Krieg, R. Caputo, C. H. Hendon, R. X. Yang, A. Walsh, M. V. Kovalenko, *Nano Lett* **2015**, 15, 3692.
- [7] Y. Shang, Y. Liao, Q. Wei, Z. Y. Wang, B. Xiang, Y. Ke, W. Lui, Z. J. Ning, Highly stable hybrid perovskite light-emitting diodes based on Dion-Jacobson structure, <https://www.science.org> (accessed: 2019).
- [8] H.-C. Wang, Z. Bao, H.-Y. Tsai, A.-C. Tang, R.-S. Liu, *Small* **2018**, 21, 1702433.
- [9] Y. Lee, J. Kwon, E. Hwang, C.-H. Ra, W. J. Yoo, J.-H. Ahn, J. H. Park, J. H. Cho, *Adv. Mater.* **2015**, 27, 41.
- [10] L. Dou, Y. Yang, J. You, Z. Hong, W.-H. Chang, G. Li, Y. Yang, *Nat. Commun.* **2014**, 5, 5404.
- [11] W. Chen, M. Zhou, Y. Liu, X. Yu, C. Pi, Z. Yang, H. Zhang, Z. Liu, T. Wang, J. Qiu, S. F. Yu, Y. Yang, X. Xu, *Adv. Funct. Mater.* **2022**, 32, 2107424.
- [12] F. Zhang, H. Zhong, C. Chen, X.-G. Wu, X. Hu, H. Huang, J. Han, B. Zou, Y. Dong, *ACS Nano* **2015**, 9, 4533.
- [13] X. Li, Z. Wen, S. Ding, F. Fang, B. Xu, J. Sun, C. Liu, K. Wang, X. W. Sun, *Adv. Opt. Mater.* **2020**, 8, 2000232.
- [14] J.-H. Im, C.-R. Lee, J.-W. Lee, S.-W. Park, N.-G. Park, *Nanoscale* **2011**, 3, 4088.
- [15] F. Liu, Y. Zhang, C. Ding, S. Kobayashi, T. Izuishi, N. Nakazawa, T. Toyoda, T. Ohta, S. Hayase, T. Minemoto, K. Yoshino, S. Dai, Q. Shen, *ACS Nano* **2017**, 11, 10373.
- [16] H. J. Snaith, *Nat. Mater.* **2018**, 17, 372.
- [17] S. F. Solari, S. Kumar, J. Jagielski, N. M. Kubo, F. Krumeich, C.-J. Shih, *J. Mater. Chem. C. Mater.* **2021**, 9, 5771.
- [18] F. Krieg, S. T. Ochsenbein, S. Yakunin, S. Ten Brinck, P. Aellen, A. Süess, B. Clerc, D. Guggisberg, O. Nazarenko, Y. Shynkarenko, S. Kumar, C.-J. Shih, I. Infante, M. V. Kovalenko, *ACS Energy Lett.* **2018**, 3, 641.
- [19] A. Jancik Prochazkova, M. C. Scharber, C. Yumusak, J. Jančík, J. Másilko, O. Brüggemann, M. Weiter, N. S. Sariciftci, J. Krajcovic, Y. Salinas, A. Kovalenko, *Sci. Rep.* **2020**, 10, 15720.
- [20] J. De Roo, M. Ibáñez, P. Geiregat, G. Nedelcu, W. Walravens, J. Maes, Z. Hens, *ACS Nano* **2016**, 10, 2071.
- [21] S. N. Habisreutinger, T. Leijtens, G. E. Eperon, S. D. Stranks, R. J. Nicholas, H. J. Snaith, *Nano Lett* **2014**, 14, 5561.
- [22] P. G. Papagiorgis, A. Manoli, A. Alexiou, P. Karacosta, X. Karagiorgis, G. Papaparaskeva, C. Bernasconi, M. I. Bodnarchuk, M. V. Kovalenko, T. Krasia-Christoforou, G. Itskos, *Front. Chem.* **2019**, 7, 87.
- [23] Y. Wei, X. Deng, Z. Xie, X. Cai, S. Liang, P. Ma, Z. Hou, Z. Cheng, J. Lin, *Adv. Funct. Mater.* **2017**, 27, 1703535.
- [24] Y. Wang, J. He, H. Chen, J. Chen, R. Zhu, P. Ma, A. Towers, Y. Lin, A. J. Gesquiere, S.-T. Wu, Y. Dong, *Adv. Mater.* **2016**, 28, 10710.
- [25] T. Xuan, J. Huang, H. Liu, S. Lou, L. Cao, W. Gan, R.-S. Liu, J. Wang, *Chem. Mater.* **2019**, 31, 1042.
- [26] J. Wu, Y. Cui, B. Yu, K. Liu, Y. Li, H. Li, J. Shi, H. Wu, Y. Luo, D. Li, Q. Meng, *Adv. Funct. Mater.* **2019**, 29, 1905336.
- [27] F. Wang, A. Shimazaki, F. Yang, K. Kanahashi, K. Matsuki, Y. Miyauchi, T. Takenobu, A. Wakamiya, Y. Murata, K. Matsuda, *J. Phys. Chem. C* **2017**, 121, 1562.
- [28] M. R. Kar, S. Kumar, T. K. Acharya, C. Goswami, S. Bhaumik, *RSC Adv.* **2023**, 13, 5946.
- [29] J. Jiang, Q. Wang, Z. Jin, X. Zhang, J. Lei, H. Bin, Z.-G. Zhang, Y. Li, S. Liu, *Adv. Energy Mater.* **2018**, 8, 1701757.
- [30] V. M. Arivunithi, S. S. Reddy, V. G. Sree, H.-Y. Park, J. Park, Y.-C. Kang, E.-S. Shin, Y.-Y. Noh, M. Song, S.-H. Jin, *Adv. Energy Mater.* **2018**, 8, 1801637.
- [31] E. Darwish, J. Elia, A. Barabash, H. Hu, M. Batentschuk, A. Osvet, *Adv. Eng. Mater.* **2024**, 26, 2400082.
- [32] F. Bisconti, A. Giuri, L. Dominici, S. Carallo, E. Quadrivi, R. Po', P. Biagini, A. Listorti, C. E. Corcione, S. Colella, A. Rizzo, *Nano Energy* **2021**, 89, 106406.
- [33] T.-H. Han, J.-W. Lee, C. Choi, S. Tan, C. Lee, Y. Zhao, Z. Dai, N. De Marco, S.-J. Lee, S.-H. Bae, Y. Yuan, H. M. Lee, Y. Huang, Y. Yang, *Nat. Commun.* **2019**, 10, 520.
- [34] H. Yang, Y. Zhang, J. Pan, J. Yin, O. M. Bakr, O. F. Mohammed, *Chem. Mater.* **2017**, 29, 8978.
- [35] H. Hu, H. Shi, J. Zhang, J. A. Hauch, A. Osvet, C. J. Brabec, *ACS Appl. Nano Mater.* **2024**, 7, 8823.
- [36] I. Levchuk, P. Herre, M. Brandl, A. Osvet, R. Hock, W. Peukert, P. Schweizer, E. Spiecker, M. Batentschuk, C. J. Brabec, *Chem. Commun.* **2017**, 53, 244.